

# Crystallite-size Dependent Harmonic Magneto-electricity in SmFeO<sub>3</sub>

Pooja Sahlot and Anand Mohan Awasthi\*

*UGC-DAE Consortium for Scientific Research, University Campus,  
Khandwa Road, Indore- 452 001, India*

\*[amawasthi@csr.res.in](mailto:amawasthi@csr.res.in)

## Abstract

First- and second-harmonic dielectric susceptibilities are maidenly studied on Samarium Orthoferrite of mesoscopic/500 nm and nanoscopic/55 nm grainsizes. Magneto-electrically coupled to the antiferromagnetic and spin-reorientation transitions, fundamental and harmonic dielectricity consistently reflect the global/local polarization effects of crystallite-size dependent electrical orderings. Bulk and incipient ferroelectricity respectively in nanoscopic and mesoscopic crystallites concur the higher-temperature antiferromagnetic ordering ( $T_N \sim 670$  K). Upon the spin-reorientation transition at lower-temperature ( $T_{SR} \sim 470$  K), re-entrant relaxor state in the nano-crystallites and bulk-like/temperature-windowed ferroelectricity in the meso-crystallites emerge. In the nano-crystallites, magneto-electric signature of interfacial spins' de-pinning ( $T_{SP} \sim 540$  K) is exclusively revealed by the scaled-harmonics.

**Keywords:** Samarium Orthoferrite, Multiferroicity, Harmonic dielectricity, Crystallite size

## Introduction

RFeO<sub>3</sub> oxides are the perovskites with rich properties and functional applicability in spintronics, magneto-electric memory, solid oxide fuel cells, and many others [1,2,3]. Perovskites and related systems with multiple magnetic phases and respective transitions have shown interesting magneto-electric properties in the literature [4,5]. In RFeO<sub>3</sub> family, samarium orthoferrite (SmFeO<sub>3</sub>; SFO) with single-phase ambient multiferroicity is of great interest [6,7]. Here, G-type antiferromagnetic ordering of Fe<sup>3+</sup> ions with weak ferromagnetism along the *c*-axis occurs below  $T_N = 670$  K [8,9]. Upon further cooling, the SFO system shows reorientation of Fe<sup>3+</sup> spins from the *c*-axis to *a*-axis below  $T_{SR} = 470$  K [10]. Fe-Sm interactions are reported to play a crucial role in this magnetostrictive transition [11]. Significant displacement of Sm-ion in the octahedra introduces (improper) polarization in SFO [12], presenting good candidate multiferroic for study.

Chaturvedi et. al. [9,13] have carried out detailed particle-size dependent study on SFO. The group witnessed magneto-dielectric coupling about  $T_N$  in SFO nanoparticles ( $\sim 55$  nm) [13], which has been attributed to exchange striction and significant intrinsic surface stress of the nanoparticle-shell. Raman measurements in the studied system evidenced spin-phonon coupling across  $T_N$  and  $T_{SR}$ . In SFO with meso-sized grains ( $\sim 500$  nm), qualitative change in the ac-conductivity mechanism across  $T_{SR}$  was reported via its Jonscher power-law analysis [9]. Interestingly, the strength and type of magneto-electric (ME) couplings about  $T_{SR}$  and  $T_N$  were observed to depend on the grain size. In this regard, we expect the nature and magnitude of ME-induced polarizations to be crystallite-size dependent, providing important functional implications. To precisely characterize the global/local polarizations and thus identify the exact electrical orderings across the temperatures of interest, we present the first upgraded dielectric study in SFO; involving the harmonic susceptibility investigations. These were demonstrated in our previous report [14], to manifest profound signatures of unusual polarizations, which decipher several variant electrically-ordered states in different perovskite-related systems.

Here, we have performed dielectric fundamental, first-, and second-harmonics study on two SFO specimens- with grains of mesoscale ( $m$ -SFO  $\sim 500$  nm) and nanoscale size ( $n$ -SFO  $\sim 55$  nm). Samarium Orthoferrite ( $\text{SmFeO}_3$ ) has orthorhombic symmetry (Pnma), with distorted  $\text{FeO}_6$  octahedra [9]. Magnetic study on the specimens found their antiferromagnetic transition ( $\text{Fe}^{3+}$  spins) at  $T_N = 670$  K and spin-reorientation at 470 K (disorder-broadened;  $\pm 10$  K)--where weak-ferromagnetic moment associated with the Fe-spins reorients from the  $c$ -axis to the  $a$ -axis [9]. Chaturvedi et. al. reported dielectric properties for  $n$ -SFO (avg. particle size  $\approx 55 \pm 5$  nm) with non-dispersive  $\epsilon'$ -peaks at  $T_N$ , wherein no sharp anomaly could be observed for  $m$ -SFO specimen [9]. From first- and second-harmonic dielectric measurements, here we present clear and profound ME-coupling driven polarization-characters across both  $T_N$  and  $T_{SR}$ , with well-distinguished magneto-harmonic effects in  $n$ -SFO and  $m$ -SFO specimens—as crystallite-size dependent non-linear dipolar-response. Further, novel magneto-electric feature across the interfacial-spins' depinning temperature ( $T_{SR} < T_{SP} < T_N$ ) is exclusively revealed from scaled-harmonic susceptibility.

## Dielectric- Fundamental and Harmonics Study on *m*-SFO (500 nm grain-size)

Fundamental dielectric measurements were performed on the *m*-SFO specimen, where fig. 1 presents temperature dependence (300-750 K) of dielectric constant  $\epsilon'(T)$  in the frequency range of 100 Hz to 100 kHz.  $\epsilon'(T)$  isochrones depict no sharp feature at  $T_N$  (670 K); upon cooling there is steep drop in loss-tangent (fig.1 (b)) and a local-plateau in  $\epsilon'(T)$  (fig.1 (a)) around ~600 K. Across the spin reorientation transition ( $T_{SR} \sim 470$ K) however, clear non-dispersive peak-anomaly shows in both dielectric-constant and loss-tangent (fig.1 (a, b)). Here, low-valued  $\epsilon'$  and losses ( $\tan\delta < 1$ ) reflect intrinsic nature of magneto-dielectric anomaly, indicating a bulk-like polarization.

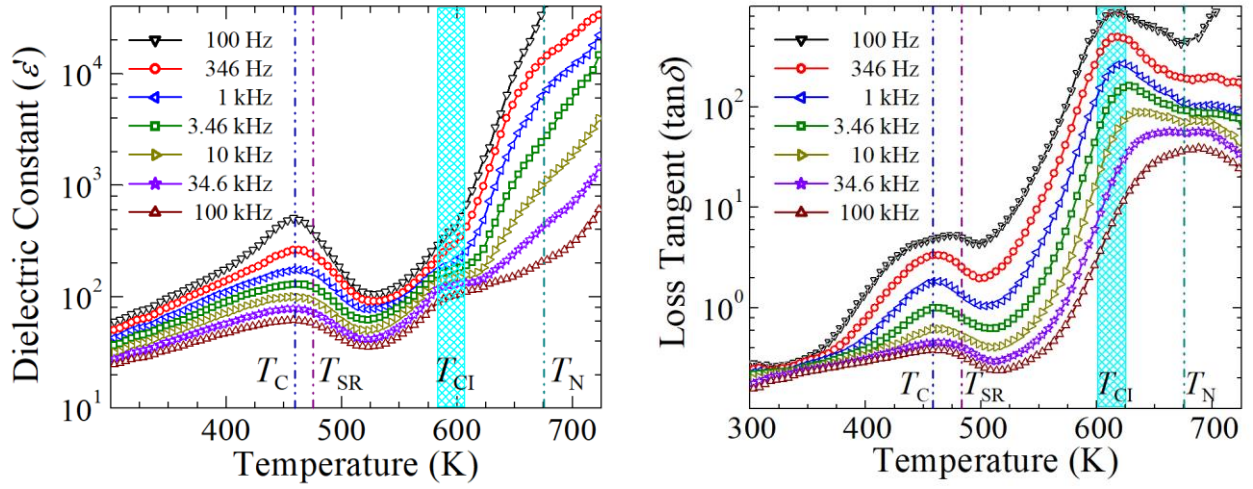


Figure 1. Temperature dependence of (a) dielectric constant ( $\epsilon'$ ) and (b) loss-tangent for *m*-SFO.

For further rigorous investigation, non-linear dielectric measurements of first- and second-order harmonics were performed across 300-750 K over (instrument-limited) frequency range of 100 Hz to 750 Hz. First and second harmonics directly probe the polarization ( $P$ ) in the system [15];

$$\epsilon'_2 = -3\epsilon_0^2 B P \chi'^3 \quad (1)$$

$$\epsilon'_3 = -(1 - 18\epsilon_0 B P^2 \chi') \epsilon_0^3 B \chi'^4 \quad (2)$$

Here,  $B$  is the positive coefficient of bipolar polarization-term ( $P^2$ ) in the free energy. Second-harmonic reflects the combined effect of bilinear-term in polarization and fundamental susceptibility ( $\chi'$ ), and competition between the two determines the nature of the second-harmonic signal. Sets of the first and second harmonics have been analyzed in [14], depicting the polarization phenomenon with temperature dependence in several perovskite-related systems.

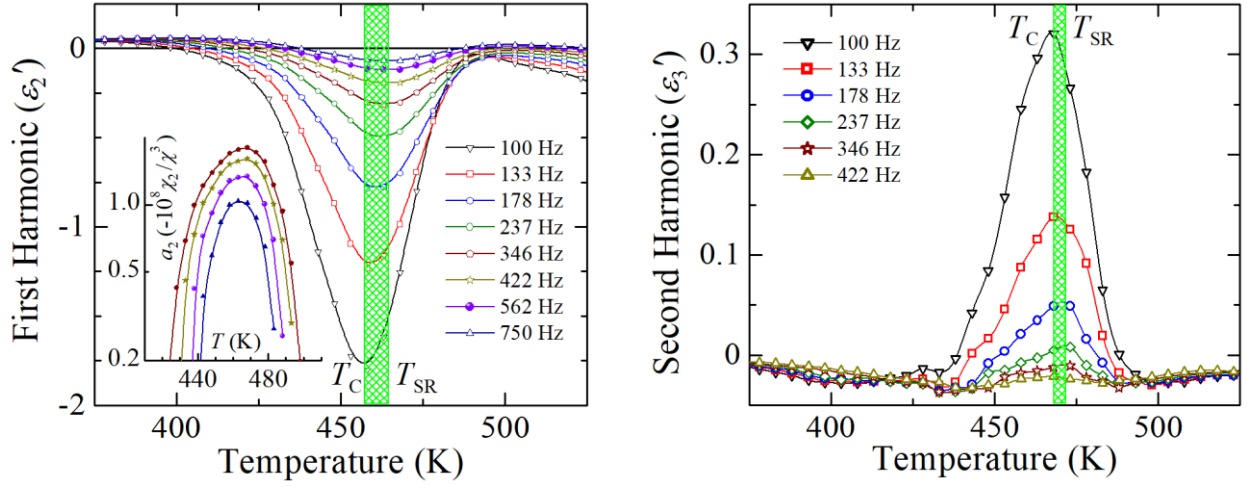


Figure 2. Temperature dependent first- and second-harmonic signals for *m*-SFO.

First- and second-harmonic susceptibilities measured for *m*-SFO system show no clear anomaly exactly at  $T_N$ . Figure 2 presents the harmonic signals-  $\varepsilon_2'(T)$  and  $\varepsilon_3'(T)$  across  $T_{SR}$ . The negative-peaks in  $\varepsilon_2'$  indicate a net polarization  $P$  (eq.1) in the system, consistent with the non-dispersive peaks in the fundamental signals (fig.1). Concurrent positive peaks in  $\varepsilon_3'$  further affirm bulk-like ferroelectricity in the mesoscopic grains, establishing a ‘Type-II’ multiferroicity, Mesoscopic-grains with ‘canted-AFM Néel-domains’ accommodate extended Néel-domain-wall, having  $c$ - to  $a$ -axis modulating spins. Advocated rather early by Kimura [16] and Mostovoy [17], symmetry-analyzed by Zvezdin [18], and lately reported e.g., in  $\text{Li}_{0.05}\text{Ti}_{0.02}\text{Ni}_{0.93}\text{O}$  [19] and  $\text{Ca}_2\text{FeCoO}_5$  [20] among others, such (short-ranged spiral/cycloidal) spin-modulations induce---via inverse Dzyaloshinskii-Moriya (ID-M) spin-orbit interaction---ME-polarization throughout the Néel-domain-wall interstitial-matrix. Effectively, this mimics ‘bulk-ferroelectricity’--- albeit existent only over the disorder-broadened  $T_{SR}$ -window, wherein the activated-process of  $c$ - to  $a$ -axis spin-reorientation occurs. The scaled first-harmonic ( $a_2(T) = -\varepsilon_2'/\chi'^3 \propto P$ ) amply evidences this in fig.2 (a)-inset, undergoing an order of magnitude rise & fall over  $\Delta T_{SR} \sim 80$  K.

Scaled  $a_2(T)$  at higher temperatures (fig. 3) depicts non-dispersive *peak* anomaly at  $\sim 600$  K. Upon cooling below  $T_N$ , losses drop sharply across this temperature (fig.1 (b)), with concurrent local-plateau in the dielectric constant (fig.1 (a)). These consistent features signify the *incipient* ferroelectric nature of the *m*-SFO system below  $T_N$ ; having only *dynamic* dipole-correlations, with their most prominent demarcating signature in the *scaled* first-harmonic signal.

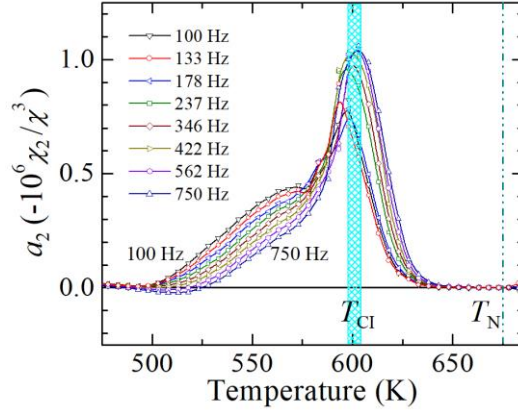


Figure 3. Scaled first-harmonic signal  $a_2(T)$ , presenting anomaly below  $T_N$  across  $\sim 600$  K.

### Dielectric- Fundamental and Harmonics Study on *n*-SFO (55 nm grain-size)

Figure 4 presents  $\varepsilon'(T)$  isochrones for the *n*-SFO specimen. In consistency with literature [9],  $\varepsilon'(T)$  shows frequency-independent peak-anomaly in the dielectric constant across  $T_N$  (fig.4 (b)). Concurrently, sharp decrease in the losses is observed, with  $\tan\delta$  dropping below 1 (fig.5), indicating intrinsic dielectric contribution below  $T_N$ . This affirms that for nano-metric grains, equivalence of crystallite-size & electrical correlation length well conserves the system's magneto-electricity across  $T_N$ . At the meso-scale, disorder comes into effect and degrades the ME-coupling at high-temperatures. Upon further cooling below  $T_{SR}$ , the bulk-like FE-correlations (well-emergent in the *m*-SFO specimen) get less-pronounced/smeared-out in the case of the *n*-SFO specimen (fig.4(a)). In consistency with the literature [13], dispersive peaks below  $T_{SR}$  in fig. 4(a) and fig. 5 correspond to the relaxor-FE state, re-entrant upon spin-reorientation, from the parent bulk ferroelectric state (realized upon the antiferromagnetic transition at  $T_N$ ).

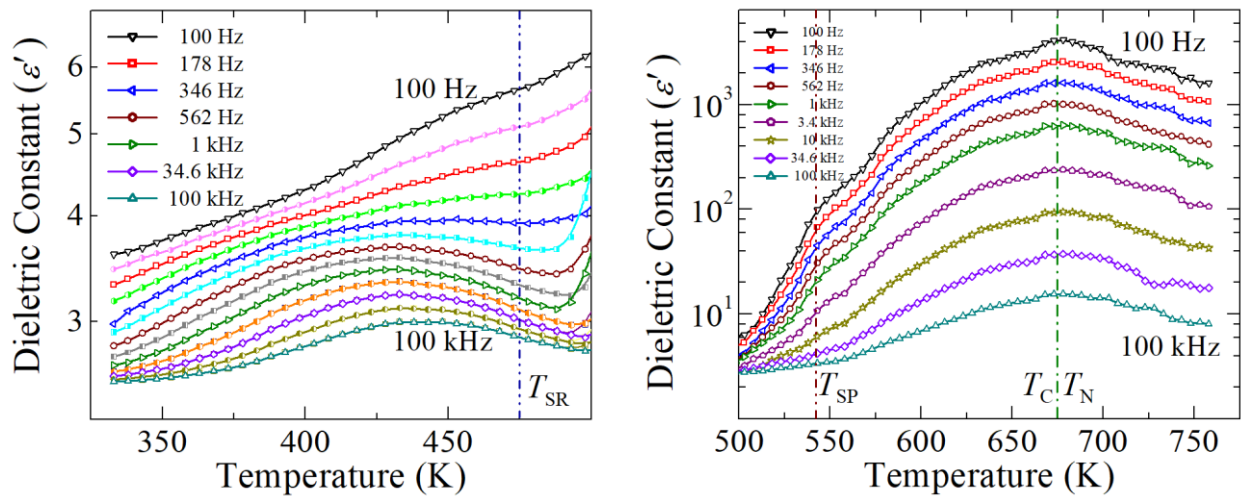


Figure 4. Temperature dependent dielectric constant for *n*-SFO across (a)  $T_{SR}$  and (b)  $T_N$ .

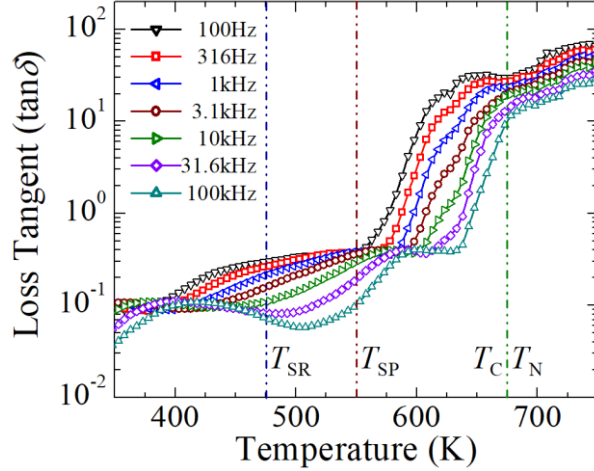


Figure 5. Temperature dependence of loss-tangent for *n*-SFO

Across  $T_N$  and  $T_{SR}$ , first- and second-harmonic measurements are performed on *n*-SFO specimen. Figure 6(a) presents negative-peaks in  $\epsilon'_2$  harmonic-signal across the AFM transition in *n*-SFO. Here, the negative anomaly in  $\epsilon'_2$  with the positive  $\epsilon'_3$ -signal across  $T_N$  (fig.6 (b)) affirm an ME-coupling induced robust polarization state. Moreover, scaled  $a_2(T)$  as a metric of the polarization  $P$ , rises by five orders of magnitude upon cooling below the  $T_N/T_C$  (fig. 6(a) inset). These consistent behaviors establish clear Type-II multiferroicity here. In the *n*-SFO specimen, although frequency-dispersive peaks in dielectric constant are observed across spin reorientation region, no anomaly-signature is present in the harmonic-signals there; both  $\epsilon'_2$ - and  $\epsilon'_3$ -signals tend to zero. Reentrant relaxor-ferroelectric state here below  $T_{SR}$  signifies Type-I multiferroicity, upon spin-reorientation.

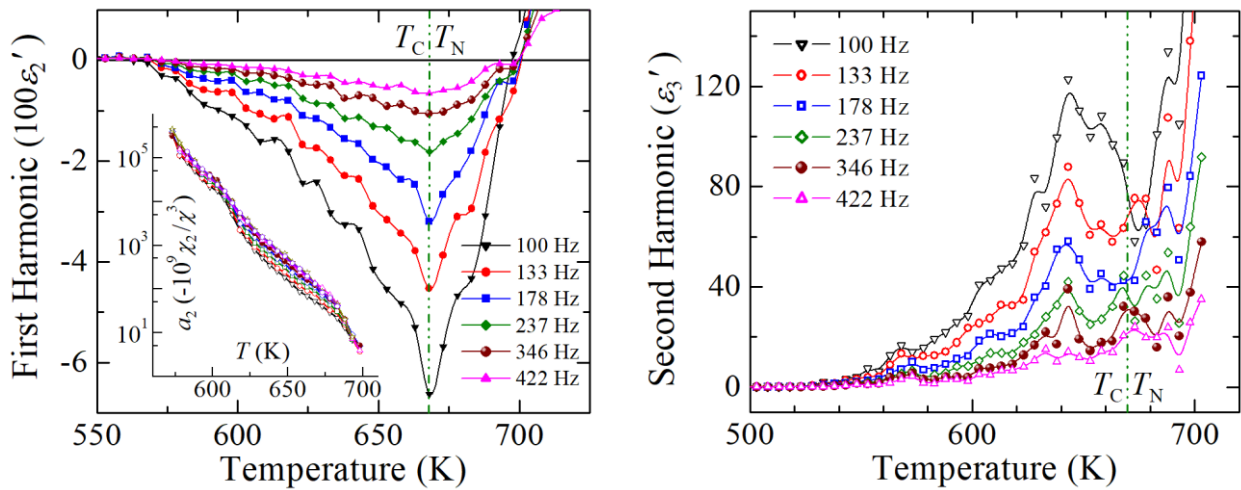


Figure 6. Temperature dependent signals of (a) first-harmonic and (b) second-harmonic in *n*-SFO.

Manifestation of hyper-polarizations ( $\varepsilon'_2, \varepsilon'_3 \neq 0$ ) requires broken electrical-isotropy (non-vanishing internal global/local fields). In the *n*-SFO specimen, the individual nanoparticles as Néel-ferrimagnetic mono-domains feature unidirectional WFM-spins throughout their entirety. The absence of Néel-wall matter to host modulating spins deprives the system of an ID-M-like mechanism for realizing domain-wall polarization, which could elicit non-linear/harmonic magneto-dielectric response over the  $T_{SR}$ -regime. Of course, the magnetic frustration---borne of spin-orientations distributed amongst the nanoparticulate Néel-domains, with its allied magneto-electric disorder---retreats the range of dipole-correlations to sub-particle-size length-scale, thereby suppressing the parent bulk ferroelectricity into a re-entrant relaxor-FE state.

Further, scaled susceptibilities evaluated as  $a_2 = -\varepsilon'_2/\chi'^3$  and  $a_3 = \varepsilon'_3/\chi'^4$  shown in fig. 7 present the temperature dependence of these scaled-harmonic signals. A pronounced anomaly is present in both the scaled susceptibilities across  $\sim 545$  K, which is not resolvable in the bare/measured harmonic-signals, and is rather extinct in the fundamental signals. In the *n*-SFO specimen, a magnetic anomaly at 550 K [9] is attributed to the thermal activation of the pinned interfacial spins in the nano-grains. Clear signature of the concurrent anomaly in scaled harmonic-susceptibilities here exclusively manifests a novel magneto-electric effect, of the subtle magnetic phenomenon in the SFO-nanoparticles, for the first time.

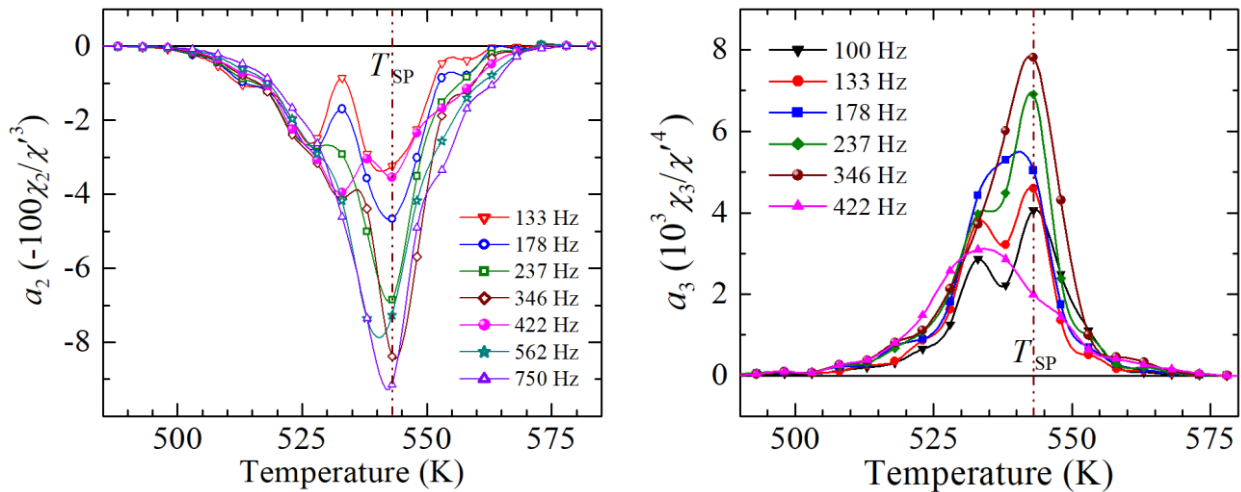


Figure 7. Temperature dependent signals of scaled parameters; (a)  $a_2(T)$  and (b)  $a_3(T)$  in *n*-SFO.

## Conclusions

Maiden first- and second-harmonic non-linear dielectric study on Samarium Orthoferrite presents novel crystallite-size dependent magneto-electric effects, obtained on mesoscopic and nanoscopic grain-sized specimen. In mesoscopic specimen, magneto-striction driven bulk-like polarization (Type-II multiferroicity) across spin-reorientation transition-window ( $\Delta T_{SR}$ ) is established, whereas around 600 K (below  $T_N$ ), clear signature of incipient ferroelectricity is affirmed by the scaled harmonic susceptibility. In nanoscopic specimen, exchange-striction and intrinsic-surface-stress driven robust ferroelectricity at  $T_N$  ( $\equiv T_C$ ; Type-II MF) is established from all-non-dispersive peak-anomalies in fundamental, first-harmonic (negative) and second-harmonic (positive) signals. Here, upon magneto-strictive spin-reorientation, the emergence of re-entrant relaxor-FE state (Type-I MF) and the absence of harmonic signals, are both traceable to the nanometric particles as Néel-ferrimagnet mono-domains---precluding the Néel-domain-wall matter and ensuing magneto-electric disorder. From scaled harmonic-signals in the nanoscopic specimen, novel magneto-electric effect marking thermal activation of interfacial-pinned spins is witnessed for the first time. Our findings reiterate the importance of harmonic dielectric investigations as exclusive upgradation tools in probing intricate/disordered polarizations and identifying complex electrical phases, which are incompletely characterized by the conventional transport parameters.

## Acknowledgments

Authors are grateful to Sulabha Kulkarni, Smita Chaturvedi, and their group-members at IISER-Pune, India, for consenting their Samarium Orthoferrite samples (*n*-SFO and *m*-SFO) for the study.



## References

---

- [1] Tokunaga, Y., Furukawa, N., Sakai, H., Taguchi, Y., Arima, T. H., & Tokura, Y. Composite domain walls in a multiferroic perovskite ferrite. *Nature Materials*, **8**(7), 558-562 (2009).
- [2] Steele, B. C., & Heinzl, A. Materials for fuel-cell technologies. In *Materials For Sustainable Energy: A Collection of Peer-Reviewed Research and Review Articles from Nature Publishing Group* (pp. 224-231) (2011).
- [3] Jeong, Y. K., Lee, J. H., Ahn, S. J., & Jang, H. M. Temperature-induced magnetization reversal and ultra-fast magnetic switch at low field in SmFeO<sub>3</sub>. *Solid state communications*, **152**(13), 1112-1115 (2012).
- [4] Sahlot, P., & Awasthi, A. M. Uncompensated-spins induced weak ferromagnetism in Ca<sub>3</sub>Mn<sub>2</sub>O<sub>7</sub>: Magneto-conductive and dual magneto-capacitive effects. *Journal of Magnetism and Magnetic Materials*, **493**, 165732 (2020).
- [5] Sahlot, P., Sharma, G., Sathe, V., Sinha, A. K., & Awasthi, A. M. Interplay of spin, lattice, vibration, and charge degrees of freedom: Magneto-dielectricity in Ca<sub>3</sub>Mn<sub>2</sub>O<sub>7</sub>. *Journal of the American Ceramic Society*, **103**(5), 3238-3248 (2020).
- [6] Maslen, E. N., Streltsov, V. A., & Ishizawa, N. A synchrotron X-ray study of the electron density in C-type rare earth oxides. *Acta Crystallographica Section B: Structural Science*, **52**(3), 414-422 (1996).
- [7] Kimel, A. V., Kirilyuk, A., Usachev, P. A., Pisarev, R. V., Balbashov, A. M., & Rasing, T. Ultrafast non-thermal control of magnetization by instantaneous photomagnetic pulses. *Nature*, **435**(7042), 655-657 (2005).
- [8] Lee, J. H., Jeong, Y. K., Park, J. H., Oak, M. A., Jang, H. M., Son, J. Y., & Scott, J. F. Spin-Canting-Induced Improper Ferroelectricity and Spontaneous Magnetization Reversal in SmFeO<sub>3</sub>. *Physical Review Letters*, **107**(11), 117201 (2011).
- [9] Chaturvedi, S., Shyam, P., Bag, R., Shirolkar, M.M., Kumar, J., Kaur, H., Singh, S., Awasthi, A.M. and Kulkarni, S. Nanosize effect: Enhanced compensation temperature and existence of magnetodielectric coupling in SmFeO<sub>3</sub>. *Physical Review B*, **96**(2), p.024434 (2017).
- [10] Belov, K. P., Kadomtseva, A. M., Krynetskii, I. B., Ocvhinnikova, T. L., Timofeeva, V. A., Pomirch, L. M., & Chervonenkis, A. Y. Transitions Due to Spin Reorientation in a Ho<sub>0.5</sub>Dy<sub>0.5</sub>FeO<sub>3</sub> Single Crystal. *JETP*, **36**, 1136 (1973).

- 
- [11] Yamaguchi, T. Theory of spin reorientation in rare-earth orthochromites and orthoferrites. *Journal of Physics and Chemistry of Solids*, **35**(4), 479-500 (1974).
- [12] Johnson, R. D., Terada, N., & Radaelli, P. G. Comment on “spin-canting-induced improper ferroelectricity and spontaneous magnetization reversal in  $\text{SmFeO}_3$ ”. *Physical Review Letters*, **108**(21), 219701 (2012).
- [13] Chaturvedi, S., Shyam, P., Apte, A., Kumar, J., Bhattacharyya, A., Awasthi, A. M., & Kulkarni, S. Dynamics of electron density, spin-phonon coupling, and dielectric properties of  $\text{SmFeO}_3$  nanoparticles at the spin-reorientation temperature: Role of exchange striction. *Physical Review B*, **93**(17), 174117 (2016).
- [14] Sahlot, P., Pandey, S., Pandey, A., & Awasthi, A. M. Harmonic magneto-dielectric study in doped-, double-, and layered-perovskites. *Journal of Applied Physics*, **127**(15), 154103 (2020).
- [15] S. Miga, J. Dec, and W. Kleemann, In *Ferroelectrics-Characterization and Modeling*, Intech Open (2011).
- [16] T. Kimura, T. Goto, H. Shintani, K. Ishizaka, T. Arima, and Y. Tokura. Magnetic control of ferroelectric polarization. *Nature* **426**, 55 (2003).
- [17] M. Mostovoy. Ferroelectricity in Spiral Magnets. *Phys. Rev. Lett.* **96**, 067601 (2006).
- [18] A. K. Zvezdin and A. A. Mukhin. Magnetolectric Interactions and Phase Transitions in a New Class of Multiferroics with Improper Electric Polarization. *JETP Letters* **88**(8), 505 (2008).
- [19] Jitender Kumar, Pankaj Pandey, and A. M. Awasthi. Magneto-dielectricity in  $\text{Li}_{0.05}\text{Ti}_{0.02}\text{Ni}_{0.93}\text{O}$  at room temperature. *Mater. Res. Express* **2**(9), 096101 (2015).
- [20] Gaurav Sharma, Shekhar Tyagi, V. R. Reddy, A. M. Awasthi, R. J. Choudhary, A. K. Sinha, and Vasant Sathe. Spin-lattice coupling mediated giant magneto-dielectricity across the spin reorientation in  $\text{Ca}_2\text{FeCoO}_5$ . *Phys. Rev. B* **99**, 024436 (2019).